



# Histomorphometric and Immunohistochemical Study Comparing the Effect of Diabetes Mellitus on the Acini of the Sublingual and Submandibular Salivary Glands of Albino Rats

Sarah Yasser<sup>1\*</sup>, Ahmed Atef Shon<sup>2</sup>

<sup>1</sup>Department of Oral Biology, Faculty of Dentistry, Tanta University, Algeish Street, Tanta City, Al Gharbeya, Egypt; <sup>2</sup>Department of Prosthodontics, Faculty of Dentistry, Gulf Medical University, Ajman, United Arab Emirates

## Abstract

**Edited by:** Ksenija Bogoeva-Kostovska

**Citation:** Yasser S, Shon AA. Histomorphometric and Immunohistochemical Study Comparing the Effect of Diabetes Mellitus on the Acini of the Sublingual and Submandibular Salivary Glands of Albino Rats. Open Access Maced J Med Sci. 2020; Mar 30; 8(A):49-54. <https://doi.org/10.3889/oamjms.2020.3722>

**Keywords:** Stereology; Submandibular salivary gland; Sublingual salivary gland; Diabetes mellitus;

Proliferating cell nuclear antigen; Oxidative stress

\***Correspondence:** Sarah Yasser, Department of Oral Biology, Faculty of Dentistry, Tanta University, Algeish Street, Tanta City, Al Gharbeya, Egypt.  
E-mail: Sarah\_a\_82@hotmail.com

**Received:** 15-Sep-2019

**Revised:** 28-Feb-2020

**Accepted:** 29-Mar-2020

**Copyright:** © 2020 Sarah Yasser, Ahmed Atef Shon

**Funding:** This research did not receive any financial support

**Competing Interests:** The authors have declared that no competing interests exist

**Open Access:** This is an open-access article distributed under the terms of the Creative Commons Attribution-NonCommercial 4.0 International License (CC BY-NC 4.0)

**AIM:** This study was designed to compare the effect of diabetes on the mucous and seromucous acini of the sublingual (SLG) and the submandibular (SMG) salivary glands of albino rats, respectively.

**METHODS:** Twenty male albino rats were assigned into two groups; control and diabetic. Three months following the induction of diabetes mellitus (DM), both the SMG and the SLG glands were removed, randomly sectioned and stained with hematoxylin and eosin to estimate the volume-weighted mean volume of the acini of both glands together with examining their morphology. Furthermore, immunohistochemistry was done to examine the expression of the proliferating cell nuclear antigen (PCNA) in both of them.

**RESULTS:** We found that, unlike the SMG acinar cells, diabetes appeared not to affect both the morphology and the volume of the SLG acini. Interestingly, PCNA expression in diabetic SMG glands acini was significantly higher than diabetic SLG glands acini. Furthermore, we found that the expression pattern of PCNA was significantly higher between the control and diabetic groups in both glands.

**CONCLUSION:** We concluded that the mucous acini of the SLG glands are less affected by the oxidative damage induced by DM.

## Introduction

Salivary glands have a key role in maintaining oral health, as they are exocrine glands that secrete saliva which is an enriched milieu composed mainly of water, electrolytes, and biologically active proteins, including growth factors and cytokines [1]. They have important functions including epithelial hydration, mastication facilitation, taste, swallowing, and speech. Furthermore, they have a buffering action with bicarbonate ions that prevent enamel decalcification while promotes remineralization.

The major salivary glands consist of paired submandibular (SMG), sublingual (SLG), and parotid glands that work simultaneously with other minor salivary glands scattered all over the oral cavity. Each one of these major salivary glands consists of a specific combination of both mucous and serous acinar cells, which are responsible for synthesizing protein components of saliva and transporting water and electrolytes [2]. A total of 1.5 L of saliva are produced by the major salivary glands: Parotid: 20–25%, SMG:

70–75%, and SLG: 5% and the rest by the minor salivary glands. Most of the resting or unstimulated saliva is from the SMG glands, while parotids contribute only to the stimulated secretions [3], [4].

Diabetes mellitus (DM) is a chronic metabolic disease that results from the failure of pancreas to produce insulin or the body cells to use this insulin. Defects in either insulin secretion or its cellular receptors cause sustained hyperglycemia, which is considered the main feature of DM and its destructive cause [5], [6].

The previous studies have focused on the physiological, pathological, and morphometrical alternations of the parotid and the SMG caused by DM [7]. However, studies on the SLG are sparse and their results are conflicting [8], [9]. This may be explained by the fact that the SLG contribution to total saliva volume is the least among all three major salivary glands. However, the SLG is still one of the major salivary glands that should undergo more detailed histological and morphometrical examination to assess DM effect. In this study, we compared the effect of DM on the acinar part of both the rat SLG and the SMG;

this was done using stereological methods, histological, and histochemical examination.

## Materials and Methods

### Animals

This study was performed on 20 adult male rats with an average body weight of 200–250 g. All animals were housed in temperature-controlled cages on a 12 h alternating light-dark cycle, for 3 months.

The protocol is designed in accordance with the guidelines for the responsible use of animals in research as a part of scientific research ethics recommendation of Research Ethics Committee, Faculty of Dentistry, Tanta University. The animals were divided into two equal groups; each group consists of 10 rats. The groups were divided into a control and a diabetic untreated group.

For DM induction, a single intraperitoneal injection of 150 mg/kg monohydrated alloxan dissolved in sterile 0.9% saline was used [10]. On the other hand, the control group was injected with sterile saline to control the effect of injection stress.

### Tissue preparations

At the end of the experimental period, rats were euthanized by cervical dislocation under general anesthesia. The SMG and the SLG of each animal were cut into small portions (3 × 3 × 3 mm). About 4% paraformaldehyde was used as a tissue fixative. To achieve random orientation of the specimens, the tissues were embedded randomly in paraffin wax [11]. The sections were cut at 5 μm intervals and stained for histological and immunohistochemical examinations using hematoxylin and eosin stain and anti-proliferating cell nuclear antigen (PCNA) antibody (Lab Vision, USA), respectively.

### Stereological study

On each cut section, five fields were selected randomly. This was done by moving the microscope's stage in horizontal and vertical directions (Leica,

Germany). We examined a total number of 95–100 acini/animal at × 400. A grid system (ImageJ) was used to estimate volume-weighted mean volume of both SMG and SLG acini using point sampled intercepts method [12], [13]. The intercept ( $I_0$ ) was measured at each point of the grid which hits an acinus by calculating the length of the line passing through this point from one side of the acinus to the opposite side in an isotropic direction. Then, the volume-weighted mean volume ( $V_v$ ) of the acini was calculated using the next equation.

$$V^v = \frac{\pi}{3} \times I_0^3 \times M. \text{ M is a correction factor}$$

calculated as  $\left(\frac{1}{Mag}\right)^3$ , where *Mag* is the microscope magnification used to examine the slides (Table 1) [14].

(A) *x* is the class number with a total number of classes *n* = 11. (B) The formula for calculation of the upper limit length<sup>3</sup> of a class number *x* is  $\frac{I_n^3}{10^{(n/n-1)}} \times 10^{(x/n-1)} - 1$ . (C) The upper limit length of

class *x* on a normal scale, the ruler length here = 25 mm. (D) The class width length<sup>3</sup> is calculated using column B, for example, the class width length<sup>3</sup> of a class *x* = upper limit length<sup>3</sup> of class *x* minus the upper limit length<sup>3</sup> of class (*x*-1). (E) Class midpoint of a class *x* = ½ class width length<sup>3</sup> of class *x* + upper limit length<sup>3</sup> of class (*x*-1). (F) The number of intercepts recorded in each class for acini of the control group. (G) The result of multiplying the midpoint lengths<sup>3</sup> by the number of intercepts recorded in each class. Column G calculates the sum of  $\sum I_0^3$ , so the calculation of volume-weighted mean volume ( $V_v$ ) of the control acini was done using the following equation:

$$V^v = \frac{\pi}{3} \times I_0^3 \times M = 1.05 \times \frac{40.83 \times 10^{14}}{94} \times \frac{1}{400^3} = 7.114 \times 10^5 \mu\text{m}^3.$$

### Immunohistochemistry

Sections were incubated with anti-PCNA antibody (mouse monoclonal primary antibody, clone PC10, Thermo Scientific Lab Vision) followed by incubation with secondary antibody (Biotinylated Goat Anti-polyvalent; Thermo Scientific Lab Vision). Following

**Table 1: The estimation of the volume-weighted mean volume ( $V_v$ ) of SMG acini of the control group using the  $I_0$  ruler**

A	B	C	D	E	F	G
Class no. X	Upper limit length <sup>3</sup> ( $\mu\text{m}^3 \times 10^{-12}$ )	Upper limit length ( $\mu\text{m} \times 10^{-4}$ )	Class width length <sup>3</sup> ( $\mu\text{m}^3 \times 10^{-12}$ )	Class midpoint ( $\mu\text{m}^3 \times 10^{-12}$ )	Observed number per class	E × F ( $\mu\text{m}^3 \times 10^{-12}$ )
1	0.35	0.7	0.35	0.18	0	0
2	0.79	0.92	0.44	0.57	0	0
3	1.34	1.1	0.55	1.07	4	4.28
4	2.04	1.27	0.7	1.69	15	25.35
5	2.91	1.43	0.87	2.48	8	19.84
6	4.02	1.59	1.11	3.47	24	83.28
7	5.41	1.76	1.39	4.72	21	99.12
8	7.16	1.93	1.75	6.29	9	56.61
9	9.36	2.11	2.2	8.26	8	66.08
10	12.13	2.3	2.77	10.75	5	53.75
11	15.62	2.5	3.49	13.88	0	0
					94	408.31

SMG: Submandibular, SLG: Sublingual.

that incubation with the appropriate percentage of DAB substrate with DAB chromogen was done until desired reaction was achieved. Finally, the slides were counterstained with hematoxylin. The results were examined using light microscope [15].

### Statistical analysis

Data were analyzed using unpaired Student's *t*-test. Results are expressed as means  $\pm$  standard deviation and  $p < 0.05$  was considered statistically significant.

## Results

### Light microscope examination

Unlike the control SMG that showed normal structures, the seromucous acini of diabetic SMG were atypical and depicted severe cytoplasmic vacuolization (Figure 1).

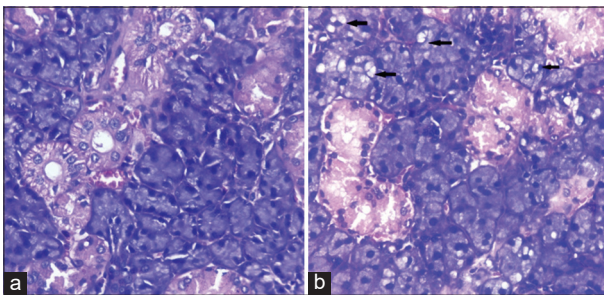


Figure 1: Light micrograph illustrates (a) the seromucous acini of control submandibular, (b) the seromucous acini of diabetic group shows severe vacuolization of the acinar cells (black arrows) (hematoxylin and eosin stain, original magnification  $\times 400$ )

However, the mucous acini of SLG were similar to those of the control group with no obvious signs of degenerative changes (Figure 2).

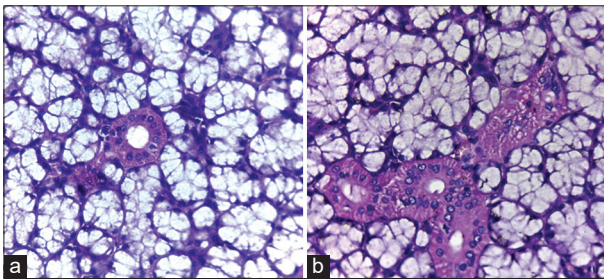


Figure 2: Light micrograph illustrates (a) the mucous acini of control sublingual, (b) the mucous acini of diabetic group shows almost no change in their morphology (hematoxylin and eosin stain, original magnification  $\times 400$ )

### Stereological study

In Table 2, we found that, 3 months after DM induction, the volume-weighted mean volume of the seromucous SMG acini showed a significant increase.

**Table 2: Changes in volume-weighted mean volume ( $\mu\text{m}^3$ ) measurements of SLG and SMG acini (values are mean  $\pm$  SD)**

Volume-weighted mean volume ( $\mu\text{m}^3$ )	SMG	SLG
Control groups	$7.11 \times 10^5 \pm 28200$	$12.39 \times 10^5 \pm 48700$
Diabetic groups	$10.30 \times 10^5 \pm 22400$	$11.97 \times 10^5 \pm 47500$

\*Control versus diabetic SMG ( $p < 0.0001$ ), control versus diabetic SLG ( $p = 0.204$ ). SMG: Submandibular, SLG: Sublingual, SD: Standard deviation.

On the other hand, the mucous SLG acini of the diabetic group showed no significant increase from the control counterpart (Figure 3).

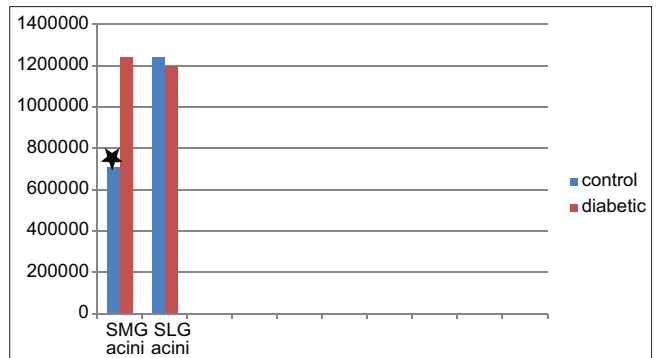


Figure 3: Changes in volume-weighted mean volume ( $\mu\text{m}^3$ ) between sublingual and submandibular acini

### Immunohistochemical study

We found in Table 3 that PCNA expression pattern did not differ significantly between control in both SMG and SLG acini. Interestingly, PCNA expression of diabetic SMG was significantly higher than diabetic SLG acini.

**Table 3: Changes in PCNA expression levels of SLG and SMG acini (values are mean  $\pm$  SD)**

PCNA expression levels	SMG	SLG
Control groups	$12.19 \pm 4.9^a$	$11.35 \pm 3.17^a$
Diabetic groups	$24.64 \pm 7.02^b$	$15.23 \pm 1.06^c$

Control versus diabetic SMG ( $p = 0.0117$ ), control SMG versus control SLG ( $p = 0.756$ ), control versus diabetic SLG ( $p = 0.032$ ), diabetic SMG versus diabetic SLG ( $p = 0.0181$ ). SMG: Submandibular, PCNA: Proliferating cell nuclear antigen, SLG: Sublingual.

Furthermore, we found that the expression pattern of PCNA was significantly higher between the control and diabetic groups in both glands (Figures 4-6).

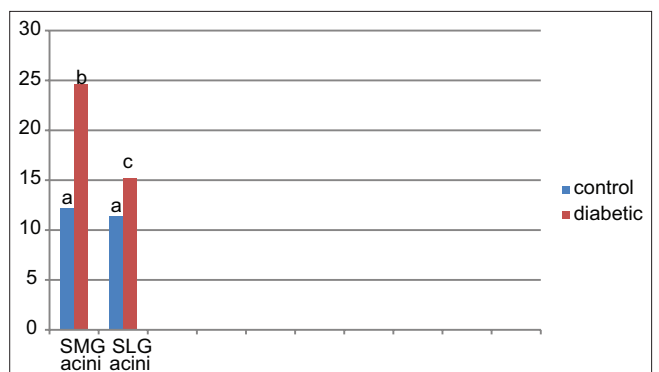


Figure 4: Changes in proliferating cell nuclear antigen expression levels of sublingual and submandibular acini (values are mean  $\pm$  standard deviation)



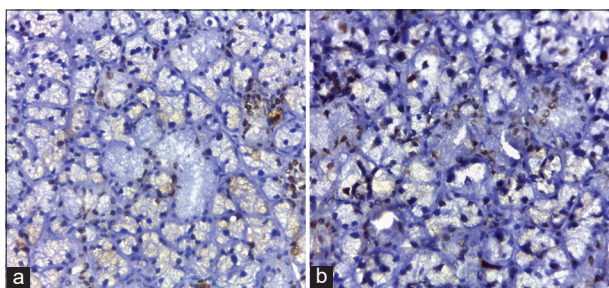


Figure 5: Light micrograph illustrates (a) positively stained acinar cells of control submandibular (SMG), (b) positively stained acinar cells of diabetic SMG (Immunoperoxidase staining of proliferating cell nuclear antigen and hematoxylin counterstain  $\times 400$ )

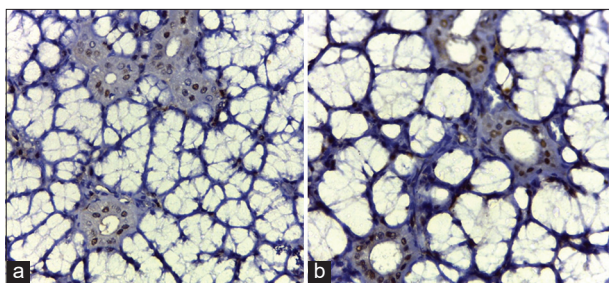


Figure 6: Light micrograph illustrates (a) positively stained acinar cells of control sublingual (SLG), (b) positively stained acinar cells of diabetic SLG (immunoperoxidase staining of proliferating cell nuclear antigen and hematoxylin counterstain  $\times 400$ )

## Discussion

In this study, we aimed to compare the deleterious effect of DM on the acinar part of both the SMG and the SLG. Like human, rat SLGs are almost purely mucous [16]. However, unlike the clear distinction between serous and mucous acini of human SMG, the nature of rat SMG was described as seromucous acini which were neither pure serous nor pure mucous [17], [18], [19].

We found that DM adversely affects the acinar part of rat SMG both qualitatively and quantitatively. Unlike the control SMG that depicted cuboidal or low columnar seromucous acini, the diabetic acini were atypical and showed significant vacuolization [20]. Sever vacuolization appeared to be a lipid nature since they were removed during fixation and processing of the samples [21].

These findings could be attributed to the destructive effect of sustained hyperglycemia that, in turn, could be contributed to oxidative stresses induction [5], [22]. These oxidative stresses are generated through several mechanisms including glucose autoxidation, activation of the polyol pathway, and formation of advanced glycation end-products (AGEs) [23]. Other circulating factors that are elevated in diabetics, such as free fatty acids and leptin, also contribute to increased reactive oxygen species generation [24].

The exact mechanism of oxidative stresses induced cell injury can be explained through indirect and direct pathways. Indirect pathways include influx of calcium from their intracellular stores and across the plasma membrane.

Increased cytosolic Ca ions activate a number of enzymes responsible for cellular damage including phospholipases, proteases, endonucleases, and adenosine triphosphatases (ATP), thereby hastening ATP depletion. This ATP depletion causes structural disruption of the protein synthetic apparatus. Furthermore, ATP depletion reduces the activity of the plasma membrane energy-dependent sodium pump, resulting in intracellular accumulation of  $\text{Na}^+$  and efflux of  $\text{K}^+$ , causing cell swelling and dilation of the ER [25]. Moreover, hyperglycemia causes impairment of sodium-glucose cotransporters, aquaporins, or both affecting cellular water content [26], [27], [28], [29]. This can explain the significant increase in the volume-weighted mean volume of the SMG seromucous acini of diabetic rats.

On the other hand, direct pathways include lipid peroxidation of the polyunsaturated membrane lipids that are vulnerable to attack by oxygen-derived free radicals. The lipid radical interactions yield peroxides, which are reactive, unstable, and endanger the integrity of cellular and nuclear membranes. This allows oxygen radicals to attack chromatin, causing fragmentation of DNA. Furthermore, free radicals react with thymine in the nuclear and mitochondrial DNA, causing single-strand breaks. This DNA damage results in cell aging and death [30].

To eradicate this DNA damage, base excision repair (BER) is activated to repair single-strand breaks and oxidized bases [31]. PCNA was found to be essential for gap filling in BER, this makes PCNA important to repair DNA lesions caused by oxidative stresses [32], this can explain the elevated level of PCNA expression in the seromucous acini of diabetic SMG, compared to the control, in an attempt to bypass the damage induced by oxidative stresses.

On the other hand, similar to earlier studies, we observed almost no changes in the cell architecture of the mucous acini of diabetic SLG; they retained their normal shape and morphology [8], [33], [34], [35]. Furthermore, we found no significant changes in the volume-weighted mean volume of mucous acini of diabetic SLG compared to the control [21]. However, PCNA expression level in the mucous acini of diabetic SLG was significantly higher than that of the control. This indicated that there are still degenerative changes caused by oxidative stresses that need to be repaired.

Interestingly, PCNA expression was higher in the diabetic compared to the control groups in both glands. However, PCNA expression was still significantly higher in seromucous acini of diabetic SMG in comparison with mucous acini of diabetic SLG. This indicated that DM adversely affected the seromucous acinar cells of SMG much more than the mucous acinar cells of SLG.

This was explained in early studies by the fact that serous acini contain secretory granules rich in proteolytic enzymes, while mucous cells do not [36], [37], [38]. Moreover, in recent studies, secretory granules of the serous acini were found to be rich in heavy metals so they are more vulnerable to metal-catalyzed attack by

free radicals and hydrogen peroxide prompted from the accumulation of AGEs [39]. Although hydrogen peroxide is not a free radical, it has the ability cross the cell membranes into different cellular compartments. Hydrogen peroxide that is not neutralized has a great affinity to react with heavy metals and forms the highly reactive hydroxyl radical (OH) which augments lipid peroxidation [40], [41].

Furthermore, the difference can be explained by the rapid intracellular lipid accumulation in serous acini, unlike the mucous acini, of diabetic salivary glands [21]. It has been suggested that lipid accumulations can be related to the reduction in the synthesis of secretory granules [30], [42], [43], [44]. This increase in free fatty acids causes increase in the production of monocyte chemoattractant protein-1 that attracts monocytes in adipose tissue and transforms them into tissue-resident inflammatory M1 phenotype macrophage [45]. This exaggerates the inflammation, resulting in a further increase in the free radicals production with subsequent weakening of the antioxidant barrier and oxidative damage to the organ [46]. In addition, Cecchini *et al.* (2009) found that Clara cell secretory protein (CC10), that has a protective effect against inflammatory response and oxidative stresses, was found exclusively in the SLGs [16].

## Conclusion

We concluded that the SMGs are much more sensitive to the deleterious effect of DM than SLGs, which are far more resistant to these damaging effects. This is mainly contributed to the nature of the acinar cells represented by the seromucous and the mucous cellular phenotype in SMGs and SLGs, respectively. The seromucous acini is more affected by the damaging effect of oxidative stresses accumulation compared to the mucous acini.

## References

- Amerongen AV, Veerman EC. Saliva-the defender of the oral cavity. *Oral Dis.* 2002;8(1):12-22. <https://doi.org/10.1034/j.1601-0825.2002.1o816.x> PMID:11936451
- Pinkstaff CA. Serous, seromucous, and special serous cells in salivary glands. *Microsc Res Tech.* 1993;26(1):21-31. <https://doi.org/10.1002/jemt.1070260104>. PMID:8219371
- Ship JA, Fox PC, Baum BJ. How much saliva is enough? "normal" function defined. *J Am Dent Assoc.* 1991;122(3):63-9. PMID:2019691
- de Almeida Pdel V, Grégio AM, Machado MA, de Lima AA, Azevedo LR. Saliva composition and functions: A comprehensive review. *J Contemp Dent Pract.* 2008;9(3):72-80. PMID:18335122
- Anderson LC, Suleiman AH, Garrett JR. Morphological effects of diabetes on the granular ducts and acini of the rat submandibular gland. *Microsc Res Tech.* 1994;27(1):61-70. <https://doi.org/10.1002/jemt.1070270105> PMID:8155905
- Nicolau J, de Matos JA, de Souza DN, Neves LB, Lopes AC. Altered glycogen metabolism in the submandibular and parotid salivary glands of rats with streptozotocin-induced diabetes. *J Oral Sci.* 2005;47(2):111-6. <https://doi.org/10.2334/josnusd.47.111> PMID:16050492
- Pinkstaff CA. Salivary glands, glycoconjugates and diabetes mellitus. *Eur J Morphol.* 1996;34(3):187-90. PMID:8874094
- Kamata M, Shirakawa M, Kikuchi K, Matsuoka T, Aiyama S. Histological analysis of the sublingual gland in rats with streptozotocin-induced diabetes. *Okajimas Folia Anat Jpn.* 2007;84(2):71-6. <https://doi.org/10.2535/ofaj.84.71> PMID:17969996
- Morris PA, Prout RE, Proctor GB, Garrett JR, Anderson LC. Lipid analysis of the major salivary glands in streptozotocin-diabetic rats and the effects of insulin treatment. *Arch Oral Biol.* 1992;37(6):489-94. [https://doi.org/10.1016/0003-9969\(92\)90105-h](https://doi.org/10.1016/0003-9969(92)90105-h) PMID:1386216
- Diniz SF, Amorim FP, Cavalcante-Neto FF, Bocca AL, Batista AC, Simm GE, *et al.* Alloxan-induced diabetes delays repair in a rat model of closed tibial fracture. *Braz J Med Biol Res.* 2008;41(5):373-9. <https://doi.org/10.1590/s0100-879x2008005000014> PMID:18488099
- Mayhew TM. Quantitative description of the spatial arrangement of organelles in a polarised secretory epithelial cell: The salivary gland acinar cell. *J Anat.* 1999;194(Pt 2):279-85. <https://doi.org/10.1046/j.1469-7580.1999.19420279.x> PMID:10337960
- Mandarim-de-Lacerda CA. Stereological tools in biomedical research. *An Acad Bras Cienc.* 2003;75(4):469-86. <https://doi.org/10.1590/s0001-37652003000400006> PMID:14605681
- Gundersen HJ, Bagger P, Bendtsen TF, Evans SM, Korbo L, Marcussen N, *et al.* The new stereological tools: Disector, nucleator and point sampled intercepts and their use in pathological research and diagnosis. *APMIS.* 1988;96(10):857-81. <https://doi.org/10.1111/j.1699-0463.1988.tb00954.x> PMID:3056461
- Yasser S. Stereological and immunohistochemical study on the submandibular gland of diabetic albino rats. *J Am Sci.* 2018;14(12):24-33.
- Yasser S, Nagy N, Marei M. *In vitro* characterization of stem cells from human exfoliated deciduous teeth (SHED). *Maced J Med Sci.* 2012;5:389-96. <https://doi.org/10.3889/mjms.1857-5773.2012.0249>
- Cecchini MP, Merigo F, Cristofaletti M, Osculati F, Sbarbati A. Immunohistochemical localization of Clara cell secretory proteins (CC10-CC26) and annexin-1 protein in rat major salivary glands. *J Anat.* 2009;214(5):752-8. <https://doi.org/10.1111/j.1469-7580.2009.01074.x> PMID:19438769
- Bocci V. Ossigeno-ozono Terapia. Milano: Casa Editrice Ambrosiana; 2000. p. 1-324.
- Bocci V. Ozone as Janus: This controversial gas can be either toxic or medically useful. *Mediators Inflamm.* 2004;13(1):3-11. <https://doi.org/10.1080/0962935062000197083> PMID:15203558
- Caldeira EJ, Camilli JA, Cagnon VH. Stereology and ultrastructure of the salivary glands of diabetic Nod mice submitted to

- long-term insulin treatment. *Anat Rec A Discov Mol Cell Evol Biol.* 2005;286(2):930-7. <https://doi.org/10.1002/ar.a.20236>  
PMid:16142810
20. Ekuni D, Endo Y, Irie K, Azuma T, Tamaki N, Tomofuji T, *et al.* Imbalance of oxidative/anti-oxidative status induced by periodontitis is involved in apoptosis of rat submandibular glands. *Arch Oral Biol.* 2010;55(2):170-6. <https://doi.org/10.1016/j.archoralbio.2009.11.013>  
PMid:20035925
  21. üyük B, Nazife S, Keleş O, Selli J, Polat E, Ünal B. Effects of diabetes on the post-menopausal rat sublingual glands: A histopathological and stereological examination. *J Exp Clin Med.* 2015;32:25-30. <https://doi.org/10.5152/eurasianjmed.2015.80>
  22. Mednieks MI, Szczepanski A, Clark B, Hand AR. Protein expression in salivary glands of rats with streptozotocin diabetes. *Int J Exp Pathol.* 2009;90(4):412-22. <https://doi.org/10.1111/j.1365-2613.2009.00662.x>  
PMid:19659899
  23. Jay D, Hitomi H, Griendling KK. Oxidative stress and diabetic cardiovascular complications. *Free Radic Biol Med.* 2006;40(2):183-92. <https://doi.org/10.1016/j.freeradbiomed.2005.06.018>  
PMid:16413400
  24. Murphy MP. How mitochondria produce reactive oxygen species. *Biochem J.* 2009;417:1-3.  
PMid:19061483
  25. Krippeit-Drews P, Kramer C, Welker S, Lang F, Ammon HP, Drews G. Interference of H<sub>2</sub>O<sub>2</sub> with stimulus-secretion coupling in mouse pancreatic beta-cells. *J Physiol.* 1999;514(Pt 2):471-81. <https://doi.org/10.1111/j.1469-7793.1999.471ae.x>  
PMid:9852328
  26. Lilliu MA, Loy F, Cossu M, Solinas P, Isola R, Isola M. Morphometric study of diabetes related alterations in human parotid gland and comparison with submandibular gland. *Anat Rec (Hoboken).* 2015;298(11):1911-8.  
PMid:26264892
  27. Delporte C. Aquaporins in salivary glands and pancreas. *Biochim Biophys Acta.* 2014;1840(5):1524-32.  
PMid:23954206
  28. Wright EM, Loo DD, Hirayama BA. Biology of human sodium glucose transporters. *Physiol Rev.* 2011;91(2):733-94.  
PMid:21527736
  29. El Sadik A, Mohamed E, El Zainy A. Postnatal changes in the development of rat submandibular glands in offspring of diabetic mothers: Biochemical, histological and ultrastructural study. *PLoS One.* 2018;13(10):e0205372. <https://doi.org/10.1371/journal.pone.0205372>  
PMid:30304036
  30. Pizzimenti S, Toaldo C, Pettazoni P, Dianzani MU, Barrera G. The "two-faced" effects of reactive oxygen species and the lipid peroxidation product 4-hydroxynonenal in the hallmarks of cancer. *Cancers (Basel).* 2010;2(2):338-63. <https://doi.org/10.3390/cancers2020338>  
PMid:24281073
  31. Meira LB, Burgis NE, Samson LD. Base excision repair. *Adv Exp Med Biol.* 2005;570:125-73.  
PMid:18727500
  32. Tsai YC, Wang YH, Liu YC. Overexpression of PCNA attenuates oxidative stress-caused delay of gap-filling during repair of UV-induced DNA damage. *J Nucleic Acids.* 2017;2017:8154646. <https://doi.org/10.1155/2017/8154646>  
PMid:28116145
  33. Ibuki FK, Simões A, Nogueira FN. Antioxidant enzymatic defense in salivary glands of streptozotocin-induced diabetic rats: A temporal study. *Cell Biochem Funct.* 2010;28(6):503-8. <https://doi.org/10.1002/cbf.1683>  
PMid:20669150
  34. Turner S, Zettler G, Arcos ML, Cremaschi G, Davicino R, Anesini C. Effect of streptozotocin on reactive oxygen species and antioxidant enzyme secretion in rat submandibular glands: A direct and an indirect relationship between enzyme activation and expression. *Eur J Pharmacol.* 2011;659(2-3):281-8. <https://doi.org/10.1016/j.ejphar.2011.03.015>  
PMid:21453698
  35. Parlak SN, Tatar A, Keles ON, Selli J, Can I, Unal B. Effects of menopause and diabetes on the rat parotid glands: A histopathological and stereological study. *Int J Med Sci Public Health.* 2014;3:749-55. <https://doi.org/10.5455/ijmsph.2014.040420146>
  36. Arnold WH, Orstavik TB, Holck M. A 4-methoxy-2-naphthylamide substrate for the histochemical localization of ester proteases in the submandibular gland of the rat. *Histochem J.* 1983;15(2):139-46. <https://doi.org/10.1007/bf01042282>  
PMid:6343305
  37. Chomette G, Auriol M, Vaillant JM, Bertrand JC, Chenal C. Effects of irradiation on the submandibular gland of the rat. An enzyme histochemical and ultrastructural study. *Virchows Arch A Pathol Anat Histol.* 1981;391(3):291-9. <https://doi.org/10.1007/bf00709161>  
PMid:7281495
  38. Shear M. Substrate film techniques for the histochemical demonstration of amylase and protease in salivary glands. *J Dent Res.* 1972;51(2):368-80. <https://doi.org/10.1177/00220345720510022401>  
PMid:4501476
  39. Levi B, Werman MJ. Long-term fructose consumption accelerates glycation and several age-related variables in male rats. *J Nutr.* 1998;128(9):1442-9. <https://doi.org/10.1093/jn/128.9.1442>  
PMid:9732303
  40. Lushchak VI. Free radicals, reactive oxygen species, oxidative stress and its classification. *Chem Biol Interact.* 2014;224:164-75. <https://doi.org/10.1016/j.cbi.2014.10.016>  
PMid:25452175
  41. Maciejczyk M, Matczuk J, Żendzian-Piotrowska M, Niklińska W, Fejfer K, Szarmach I, *et al.* Eight-week consumption of high-sucrose diet has a pro-oxidant effect and alters the function of the salivary glands of rats. *Nutrients.* 2018;10(10):E1530. <https://doi.org/10.3390/nu10101530>  
PMid:30336621
  42. Mahay S, Adeghate E, Lindley MZ, Rolph CE, Singh J. Streptozotocin-induced Type 1 diabetes mellitus alters the morphology, secretory function and acyl lipid contents in the isolated rat parotid salivary gland. *Mol Cell Biochem.* 2004;261(1-2):175-81. <https://doi.org/10.1023/b:mcbi.0000028753.33225.68>  
PMid:15362501
  43. Iaremenko AI, Kutukova SI. Experimental substantiation of hormone replacing therapy by estrogens in treatment and prevention of inflammatory infectious diseases of maxillo-facial region. *Stomatologija (Mosk).* 2007;86(6):13-7  
PMid:18163096
  44. Yashida MH, Da Silva Faria AL, Caldeira EJ. Estrogen and insulin replacement therapy modulates the expression of insulin-like growth factor-I receptors in the salivary glands of diabetic mice. *Anat Rec (Hoboken).* 2011;294:1930-8 <https://doi.org/10.1002/ar.21481>
  45. Solinas G, Karin M. JNK1 and IKKbeta: Molecular links between obesity and metabolic dysfunction. *FASEB J.* 2010;24(8):2596-611. <https://doi.org/10.1096/fj.09-151340>  
PMid:20371626
  46. Iervolino A, De La Motte LR, Petrillo F, Proserpi F, Alvino FM, Schiano G, *et al.* Corrigendum: Integrin beta 1 is crucial for urinary concentrating ability and renal medulla architecture in adult mice. *Front Physiol.* 2018;9:1676. <https://doi.org/10.3389/fphys.2018.01676>  
PMid:30546318